

Spin crossover Fe^{II} complexes as templates for bimetallic oxalate-based 3D magnets

Eugenio Coronado ^{a,*}, José R. Galán Mascarós ^{a,*}, Mari Carmen Giménez-López ^a,
Manuel Almeida ^b, João C. Waerenborgh ^b

^a Instituto de Ciencia Molecular, Universidad de Valencia, Polígono de la Coma, s/n, E-46980 Paterna, Spain

^b Dept. Química, ITN/CFMC-UL, P-2686-953 Sacavém, Portugal

Abstract

We present the synthesis and structural characterization of the salt [Fe(bpp)₂][MnCr(ox)₃]₂ • bpp • CH₃OH. It crystallizes in the monoclinic space group. This material contains an anionic [MnCr(ox)₃]⁻ 3D 10-gon ferromagnetic network, that orders below 3.0 K. The channels created by this architecture are filled by the spin crossover cations [Fe(bpp)₂]²⁺ (bpp = 2,6(bispyrazol-3-yl)pyridine), free ligand and solvent molecules. No spin transition has been observed at ambient pressure.

Keywords: Coordination chemistry; Molecular materials; Spin crossover; Magnetic properties; Mössbauer spectroscopy

1. Introduction

The families of molecule-based magnets built from polymeric bimetallic oxalate complexes represent one of the most explored series in the search for molecule-based magnets. One of the key reasons is the synthetic control reached over the lattice dimensionality. Indeed, bimetallic dimers [1], trimers [2], tetramers [3], 1D chains [4], and extended 2D [5,6] and 3D lattices [7,8] have been reported from essentially the same building blocks, where the counterion and synthetic conditions dictate the formation of a given oxalate-bridged structure. Magnetic ordering has been observed in dimensionalities 1 or higher.

Ferromagnetic bimetallic anionic chains [K(18-crown-6)]-[Mn(H₂O)₂Cr(ox)₃] are formed in the presence of flat monocationic complexes of alkali metals with crown-ether ligands [4]. Ferromagnetic interchain interactions yield ferromagnetic ordering below 3.5 K, due to the short proxim-

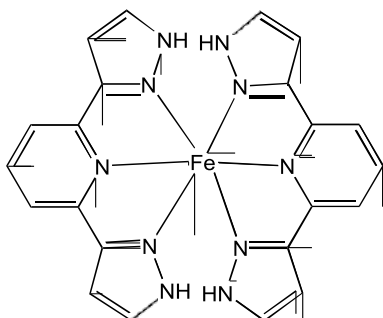
ity between these chains in the solid state, where they appear related by hydrogen bonding. These same cations, in different synthetic conditions, can also yield anionic 2D networks [K(18-crown-6)]₃[Mn₃(H₂O)₄{Cr(ox)₃]₃] where the presence of water molecules as ligands induces the formation of a distorted honeycomb network [9]. The onset of ferromagnetic ordering is observed below 4 K.

The formation of anionic 2D hexagonal networks of formula [M^{II}M^{III}(ox)₃]⁻ (M^{II} = Mn, Fe, Co, Ni, Cu; M^{III} = Cr, Fe, Ru, Rh) [5,10,11] is promoted by the use of bulky organic monocations of the tetraalkylammonium type. In these layers, where only oxalate ligands are present to achieve maximum magnetic connectivity, the metal centers show alternating chirality. Ferro- or ferrimagnetic ordering with critical temperatures up to 44 K and coercive fields over 2 T, have been reported in this series.

Chiral octahedral trischelated complexes, on the other hand, promote the formation of homochiral 3D anionic networks of the same formula, with critical temperatures much lower than those of their 2D counterparts [12]. This has been related to the weaker magnetic interactions present in this case promoted by a different relative orientation

* Corresponding author. Tel.: +34 963544420; fax: +34 963543273.

E-mail addresses: eugenio.coronado@uv.es (E. Coronado), jose.r.galan@uv.es (J.R. Galán Mascarós).



Scheme 1.

of the magnetic orbitals and to larger metal to metal distances. Most of these compounds show T_c 's below 3 K, with few exceptions reaching up to 6 K.

The use of "electroactive" cations, instead of the electronically "innocent" ones in the formation of such anionic networks has been one of the most successful approaches to multifunctional materials, where unprecedented multifunctional magnets have been obtained, such as ferromagnetic molecular metals [13,14], chemically-built magnetic multilayers [15], photoactive magnets [16], or chiral magnets [7,8,17]. Most of these examples are built from the hexagonal 2D honeycomb $[M^II M^III(ox)_3]^-$ networks. The 3D analogs have been much less explored on this regard, probably due to the more synthetically strict conditions needed. Spin crossover complexes [18] and other cations with interesting photophysical properties [19] have been embedded into these 3D systems, but including diamagnetic alkali metals in the network, preventing the appearance of magnetic ordering.

We have been investigating for several years the possibility to use Fe^II complexes as templates for oxalate-based magnets. Until now, all our attempts yielded the highly insoluble salts $[A^I][Fe(L)_3][M^III(ox)_3] \cdot xH_2O$ ($A = Li, Na, K, NH_4^+$ [20]). These compounds exhibit indeed spin crossover behavior, but no magnetic ordering is observed, since the paramagnetic centers are isolated from one another in the structure. Here we report how the complex $[Fe(bpp)_2]^{2+}$ (Scheme 1); $bpp = 2,6$ (bis(pyrazol-3-yl)pyridine) that exhibits spin crossover behavior in other simple salts [21] including the LIEST effect [22], is able to be used as cationic guest for bimetallic oxalate-based 3D magnets.

2. Experimental

2.1. Synthesis

All reagents were commercially available and used without further purification. The precursor $Ag_3Cr(ox)_3 \cdot 3H_2O$ was prepared by metathesis in water from $K_3Cr(ox)_3 \cdot 3H_2O \cdot Ag_3Cr(ox)_3 \cdot 3H_2O$ (0.098 g, 0.142 mmol) was suspended in 7.5 mL methanol, and then a solution of $MnCl_2 \cdot 4H_2O$ (0.042 g, 0.213 mmol) in 7.5 mL methanol was added dropwise. The white $AgCl$ precipitate formed was filtered, and the green solution was added to a red

solution of $Fe(ClO_4)_2 \cdot H_2O$ (0.090 g, 0.355 mmol) and bpp (0.149 g, 0.71 mmol) in 15 mL of hot MeOH. This solution was refluxed for 2 h. The yellowish precipitate formed was hot filtered, and washed with methanol and acetone. This powder was dissolved in DMF and crystals of $[Fe(bpp)_2][MnCr(ox)_3]_2 \cdot bpp \cdot CH_3OH$ (1) were grown from layering this solution with acetone. Yield: 30%. IR (cm^{-1}): 3427, w; 3124, w; 2929, w; 1654, s; 1652, s; 1628, m; 1629, m; 1462, m; 1384, m; 1277, m; 906, w; 811, w; 669, s; 541, m; 478, m; 414, m. $Mn_2N_{15}O_{25}Cr_2FeC_{46}H_{31}$, $M_w = 1463.59$. Elemental Anal. Calc.: C, 37.75; H, 2.13; N 14.36. Found: C, 37.12; H, 2.45; N, 15.20%. Desolvation of the sample was carried out by heating the crystals in air at 125 °C for 6 h.

2.2. Structural characterization

A reddish prismatic single crystal of 1 was fixed on a glass fiber and mounted on a Kappa CCD diffractometer equipped with graphite-monochromated Mo K α radiation ($k = 0.71073 \text{ \AA}$). Cell refinements and data reduction were performed at 150 K using the DENZO and SCALEPACK programs [23]. The structure was solved by direct methods using the SIR97 program [24] and refined on F^2 with the SHELXL-97 program [25]. All atoms belonging to the anionic network were located by successive Fourier transform routines, and refined anisotropically. The cations and solvent molecules, occupying the wholes left in the structure, could not be located due to the presence of severe crystallographic disorder. Two crystallographic independent positions for the Fe centers were found, with partial occupancy. Only the first coordination sphere of N atoms could be located. No good model for these complexes and solvent molecules, including the interstitial bpp moiety could be found due to heavy disorder. Crystal, data collection, and refinement parameters are summarized in Table 1.

Table 1
Crystallographic data and refinement parameters for $[Fe(bpp)_2][MnCr(ox)_3]_2 \cdot bpp \cdot CH_3OH$ (1)

Space group	monoclinic, $P2_1/n$
a (Å)	21.0100(3)
b (Å)	15.9880(4)
c (Å)	21.9630(6)
β (°)	90.3390(7)
V (Å ³)	7377.4(3)
Z	4
ρ_{calc} ($g \cdot cm^{-3}$)	1.318
T (K)	150(2)
λ (Å)	0.71073
2θ (°) range	5.88 < 2θ < 36.08
Total reflections/unique parameters	19091/4965
$R[I > 2\sigma(I)]$	0.1281, $wR_2^b = 0.3350$
$\Delta\rho_{max}/\Delta\rho_{min}$ ($e \text{ \AA}^{-3}$)	0.854/−0.386

$$^a R_1 = \frac{\sum(F_o - F_c)}{\sum(F_o)}$$

$$^b wR_2 = \frac{[\sum[w(F_o^2 - F_c^2)]/[\sum[w(F_o^2)]]^{1/2}}{P}; w = 1/[\sigma^2(F_o^2) + (0.2P)^2], \text{ where } P = (F_o^2 + 2F_c^2)/3.$$

Table 2

Estimated parameters for low-spin and high-spin Fe^{II} from the Mössbauer spectra taken at different temperatures of recrystallized [Fe(bpp)₂][MnCr(ox)₃]₂ before and after heat treatment

T (K)		Crystals				Desolvated sample			
		IS	QS	C	I (%)	IS	QS	C	I (%)
297	Fe L.S.	0.39	0.73	0.57	73	0.36	0.78	0.54	80
	Fe H.S.	1.01	2.53	0.39	27	0.97	2.34	0.36	20
120	Fe L.S.	0.49	0.78	0.49	64	0.45	0.77	0.46	73
	Fe H.S.	1.10	3.11	0.33	36	1.11	2.63	0.48	27
4	Fe L.S.	0.50	0.78	0.62	58	0.49	0.74	0.50	67
	Fe H.S.	1.15	3.25	0.35	42	1.20	2.80	0.50	33

IS (mm/s) isomer shift relative to metallic α -Fe at 295 K; QS (mm/s) quadrupole splitting; C (mm/s) line-width; I relative area. Estimated errors 60.02 mm/s for IS, QS, C, and < 2% for I.

2.3. Magnetic characterization

Bulk magnetization measurements were carried out on grained polycrystalline samples with a Quantum Design magnetometer with an applied field of 1000 G (0.1 T) in the temperature range 2–300 K, with cooling and warming cycles. AC data was collected in the 2–10 K range with an alternating field of 3.95 G ($3.95 \cdot 10^{-4}$ T) with frequencies between 1 and 1000 Hz. Hysteresis loops at 2 K were collected between 5 and –5 T. Data were corrected for diamagnetic contributions calculated using the Pascal constants.

2.4. Mössbauer spectroscopy

Mössbauer spectra were collected at different temperatures in transmission mode using a conventional constant-acceleration spectrometer and a 25 mCi ⁵⁷Co source in a Rh matrix. The velocity scale was calibrated using α -Fe foil. Isomer shifts (IS, Table 2) are given relative to metallic α -Fe at room temperature. Low-temperature spectra were collected using a JANIS bath cryostat. The spectra were fitted to Lorentzian lines using a non-linear least-squares method [26]. The relative areas and widths of both peaks in a quadrupole doublet were kept equal during refinement.

3. Results and discussion

3.1. Synthesis and structure

The insertion of the spin crossover cation [Fe(bpp)₂]²⁺ as guest into oxalate-based bimetallic networks had to start by overcoming the precipitation of the kinetic product [A^I][Fe(bpp)₂][M^{III}(ox)₃] \cdot xH₂O. This was done following the procedure used in the preparation of other oxalate bimetallic complexes avoiding the presence of any other cations in solution but the transition metal themselves. However, when a solution of Mn₃[Cr(ox)₃]₂ is treated with any salt of [Fe(bpp)₂]²⁺, again, an undesired precipitate is obtained. This material could not be structurally character-

ized. The 2:2:1 ratio found for Fe:Cr:Mn by analysis and the paramagnetic behavior suggest that maybe it is formed by oxalate-bridged trimers [2]. If the same reaction is carried out under reflux conditions for several hours this initial precipitate slowly redissolves to yield a second product, where no traces of this first compound can be found. The main component of this precipitate can be isolated by layering a DMF solution with acetone, to yield a crop of single crystals of [Fe(bpp)₂][MnCr(ox)₃]₂ \cdot bpp \cdot CH₃OH (1).

The structure of 1 is built from an anionic 3D polymeric oxalate-bridged bimetallic structure. As in the well-known chiral 3D networks, this anionic structure is formed by bis-chelating oxalate ligands that connect each divalent metal to three trivalent metals, and vice versa, building ten-membered rings in a (10,3) topology (Fig. 1). The big difference with the reported chiral 3D networks is that, in this case, the compound is achiral. Actually, it belongs to the centrosymmetric monoclinic *P*2₁/*n* space group, with metal centers of both chiralities present. This is somehow surprising because it was discussed in the past that only homochiral networks would be able to adopt such a 3D structure.

In this case, Mn(II) and Cr(III) occupy crystallographically different positions, since they are non-equivalent, and can be clearly distinguished attending to the M–O distances. The metal position with longer distances is assigned to Mn^{II}–O (2.05(3)–2.28(3) Å), and the other to Cr^{III}–O (1.94(3)–2.04(3) Å). There are two crystallographically independent Mn and Cr positions in the asymmetric unit, each one belonging to a different chirality, that are bridged together through heterochiral connections. Thus, if we con-

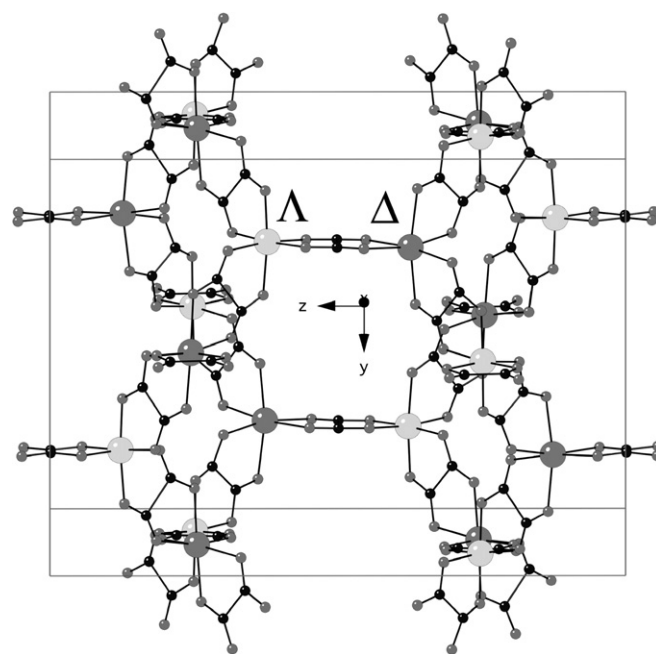


Fig. 1. Two 10-membered rings in the structure of [Fe(bpp)₂][MnCr(ox)₃]₂ · bpp · CH₃OH (1) of opposite chirality, connected along the *c* direction.

sider the rings perpendicular to the a and b axis, these are formed by five adjacent units of one chirality and opposite to that of the other five. The projections of this achiral 3D structure on the ac and bc planes are almost identical to those of the well-known chiral 3D analogs (Fig. 2), where all three projections (ab , bc , and ac) are identical. On the contrary, the projection on the ab plane for compound 1 now shows an eclipsed disposition of the rings (Fig. 3). This can be understood as a relative movement of the rings on this plane to allow for the heterochiral junctions between homochiral rings.

The electron density inside this 3D network could not be assigned to a good chemical model, due to the presence of important crystallographic disorder. One reason for this, when compared with the chiral 3D analogs, is the much higher present of interstitial solvent molecules, since only

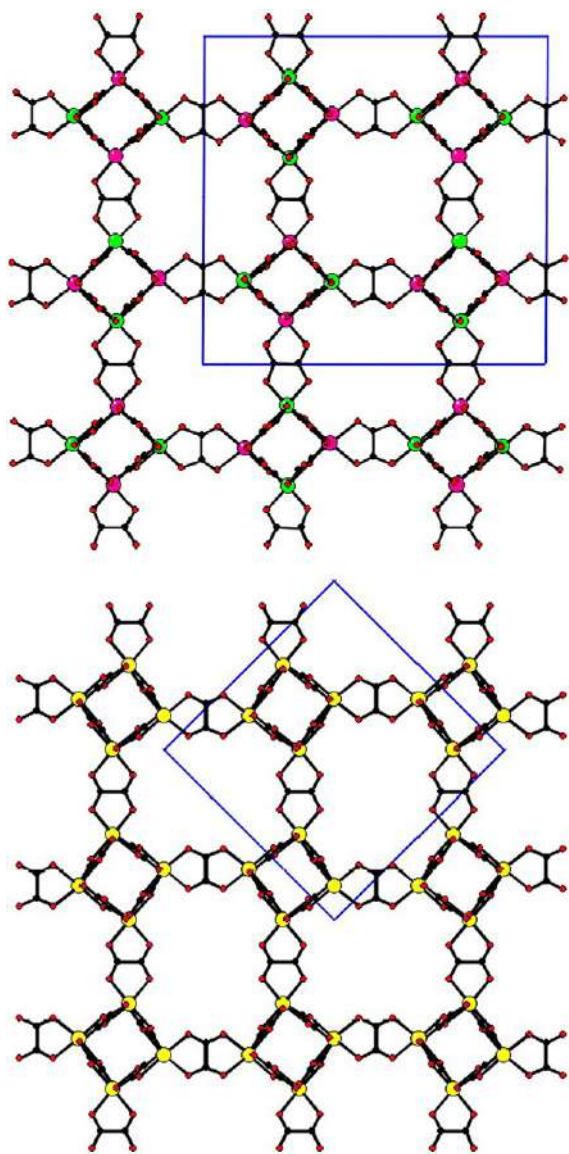


Fig. 2. Projections of the crystal structure of $[\text{Fe}(\text{bpp})_2][\text{MnCr}(\text{ox})_3]_2 \cdot \text{bpp} \cdot \text{CH}_3\text{OH}$ (top) and $[\text{Ru}(\text{bpy})_2][\text{MnCr}(\text{ox})_3]_2 \cdot \text{bpp} \cdot \text{CH}_3\text{OH}$ [7](bottom) on the bc plane.

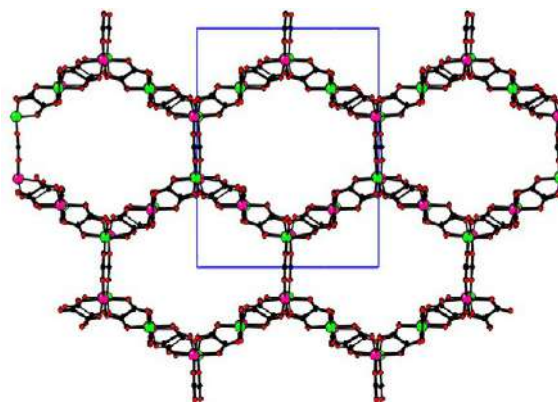


Fig. 3. Projections of the crystal structure of $[\text{Fe}(\text{bpp})_2][\text{MnCr}(\text{ox})_3]_2 \cdot \text{bpp} \cdot \text{CH}_3\text{OH}$ on the ab plane.

one Fe complex is present per MnCr pair, and therefore no extra anions are needed as in those. The cationic complexes occupy analogous positions in the crystal structure, but now with half occupancy, since this positions are shared with disordered solvent and free bpp moieties. With the data obtained, only the position for the Fe atoms, including the first coordination sphere of six N atoms could be located.

3.2. Magnetic properties

With exception of the achiral nature of this network, the connectivity between the metals is identical to that of the chiral 3D bimetallic magnets described before and thus, the magnetic properties were expected to be analogous, with the addition of the magnetic behavior of the embedded Fe^{II} complexes. The thermal dependence of the $v_m T$ product (Fig. 4) shows a small but continuous decrease when cooling down the sample. Since the interactions

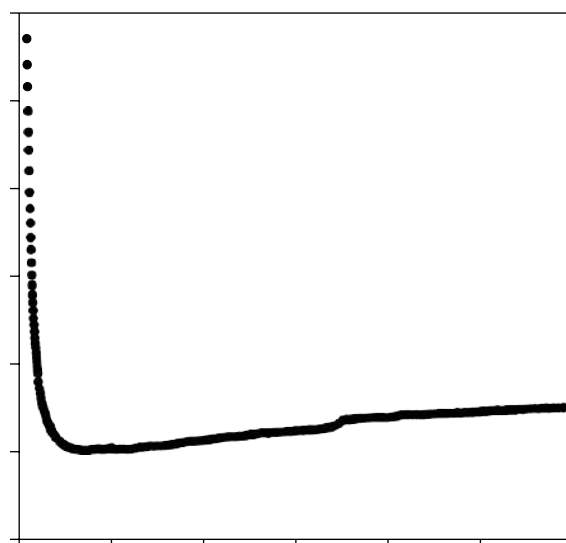


Fig. 4. Thermal dependence of the vT product for $[\text{Fe}(\text{bpp})_2][\text{MnCr}(\text{ox})_3]_2 \cdot \text{bpp} \cdot \text{CH}_3\text{OH}$.

between Mn^{II} and Cr^{III} centers promoted by the oxalate bridge are expected to be ferromagnetic, this behavior suggests a slow and non-cooperative spin transition for the Fe centers, between high spin (HS) and low spin (LS) configurations. The high temperature regime can be fitted to a Curie Weiss law with a Curie constant of $15.49 \text{ emu K mol}^{-1}$, in perfect agreement with the spin only expected value for a magnetically diluted sample. At 300 K the $\nu_m T$ is $15.05 \text{ emu K mol}^{-1}$. This suggests that around 15% of the Fe centers are LS at this temperature. The $\nu_m T$ product reaches a minimum at 35 K ($14.03 \text{ emu K mol}^{-1}$) and starts to increase rapidly, due to the ferromagnetic interaction in the network, and suggesting the presence of magnetic ordering at very low temperatures.

AC susceptibility magnetic data (Fig. 5) confirm the onset of ferromagnetic ordering below 3.0 K, with an appearance of a frequency independent out-of-phase signal, accompanying a maximum in the in-phase signal. This temperature is in good agreement with that found for other 3D $[\text{MnCr}(\text{ox})_3]^-$ networks, where ferromagnetic ordering is achieved up to 3.9 K [7]. The appearance of ferromagnetic ordering was also confirmed by zero field cooled and field cooled DC measurements at very low applied magnetic fields that deviate from one another at this very same temperature.

The field dependence of the magnetization in the ordered state at 2 K (Fig. 6) shows a very fast increase at low fields and then tends to saturation, although it is not reached even at 5 T, with a value of $15.06 \mu_B$. This is very close to the $16 \mu_B$ expected for ferromagnetic alignment of the Mn and Cr centers in the network, and confirms that the magnetic ordering is indeed of ferromagnetic nature. No clear contribution of the Fe centers is found, what suggests that at this temperature most of the Fe centers will be in their LS configuration.

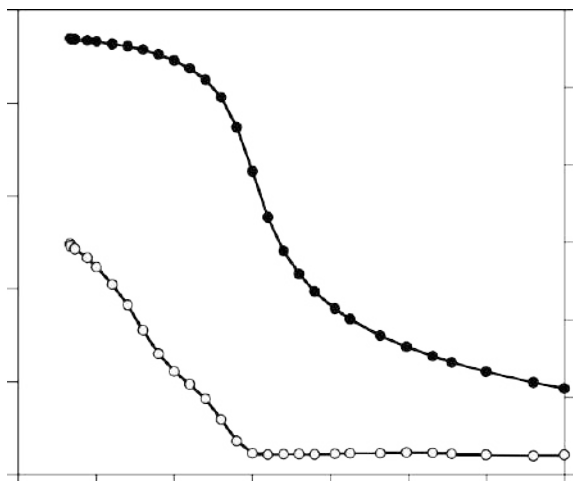


Fig. 5. Thermal dependence of the AC in-phase (χ'' , full circles) and out-of-phase (χ'' , empty circles) magnetic susceptibilities for $[\text{Fe}(\text{bpp})_2][\text{MnCr}(\text{ox})_3]_2 \cdot \text{bpp} \cdot \text{CH}_3\text{OH}$ at 333 Hz.

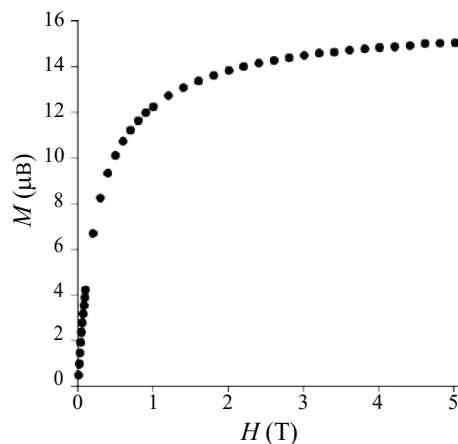


Fig. 6. Field dependence of the magnetization at 2 K for $[\text{Fe}(\text{bpp})_2][\text{MnCr}(\text{ox})_3]_2 \cdot \text{bpp} \cdot \text{CH}_3\text{OH}$ at 333 Hz.

Since desolvation usually affects the spin crossover behavior, we also performed DC magnetic measurements on desolvated samples. We found that the behavior is essentially identical, while the $\nu_m T$ product is slightly lower, indicating that desolvation increases the population of LS Fe^{II} , but it does not affect qualitatively the thermal magnetic behavior of the sample.

3.3. Mössbauer spectroscopy

All the Mössbauer spectra (Fig. 7) may be fitted with two quadrupole doublets. The estimated parameters (Table 2) for the doublet with the largest quadrupole splitting, QS, are typical of HS Fe^{II} with $S = 2$ [27]. The significantly lower QS and IS as well as the temperature independent

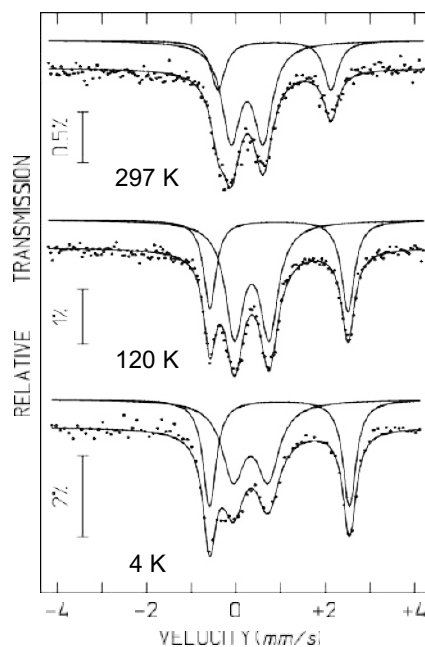


Fig. 7. Mössbauer spectra for $[\text{Fe}(\text{bpp})_2][\text{MnCr}(\text{ox})_3]_2 \cdot \text{bpp} \cdot \text{CH}_3\text{OH}$ at different temperatures.

QS of the other doublet are consistent with LS Fe^{II}, $S = 0$. After heat treatment, QS and the peak widths estimated for HS Fe^{II} change significantly (Table 2). Furthermore estimated relative areas indicate a stabilization of the LS relative to the HS state after desolvation.

If the recoil-free fractions of both HS and LS Fe^{II} are similar in the measured temperature range a much unexpected conclusion is derived: the fraction of Fe^{II} in the HS state significantly decreases with increasing temperature for both untreated and heat-treated samples. As far as we know, such a result has never been reported. A more detailed investigation is however necessary as the observed difference in the temperature dependencies of the HS and LS Fe^{II} relative areas may be due to much stronger chemical bonds established by HS Fe^{II} than by LS Fe^{II}. This would imply a stronger decrease with increasing temperature of the recoilless factor of the LS Fe^{II} as compared to HS Fe^{II}.

4. Conclusions

We have shown how it is possible to obtain molecule-based magnets based on bimetallic oxalate complexes using as template the spin crossover complex [Fe(bpp)₂]²⁺. The compound [Fe(bpp)₂][MnCr(ox)₃]₂ · bpp · CH₃OH shows ferromagnetic ordering below 3.0 K. From the structural point of view, this is the first achiral polymorph to the well-known chiral 3D cubic structure [Z(L)₃][ClO₄]-[MnCr(ox)₃] (Z = Ru, Fe; L = 2,2'-dipyridyl). It was discussed in the past that the extra perchlorate anions were needed to obtain this type of salts. Now we have also demonstrated that this is not true, and these magnets can also be obtained by substitution of half of the cations by solvent molecules. This lower occupancy of cations and anions inside the anionic network could be responsible for losing the enantiopure character of these systems.

The [Fe(bpp)₂]²⁺ units embedded in this oxalate network are not showing a clear spin transition. Apparently, LS and HS centers co-exist at all temperatures. Magnetic measurements suggest that there is a small decrease in the HS population when the temperature is decreased, that would be responsible for the lowering of the magnetic moment. On the other hand, Mössbauer spectra do not support this hypothesis. They suggest quite the opposite, if recoil-free fractions of LS and HS Fe^{II} are assumed to be similar. At this moment there is no satisfactory explanation for these apparently contradictory data. In any case, although magnetic ordering is achieved, the lack of cooperative spin transition in this compound precludes the study of possible synergy between both processes. Other spin crossover complexes, able to better fill the holes in such structural motif would probably be better candidates in the search for such a material.

Acknowledgements

This work was supported by the European Union (Network of Excellence: MAGMANET). Financial sup-

port from the Ministerio de Educación y Ciencia (Projects MAT2004-3849 and BQU2002-01091), and from the Generalitat Valenciana (GV04A/77) is also acknowledged.

Appendix A. Supplementary material

CCDC 618990 contains the supplementary crystallographic data for this paper. These data can be obtained free of charge via <http://www.ccdc.cam.ac.uk/conts/retrieving.html>, or from the Cambridge Crystallographic Data Centre, 12 Union Road, Cambridge CB2 1EZ, UK; fax: (+44) 1223-336-033; or e-mail: deposit@ccdc.cam.ac.uk. Supplementary data associated with this article can be found, in the online version, at [doi:10.1016/j.poly.2006.09.064](https://doi.org/10.1016/j.poly.2006.09.064).

References

- [1] S. Triki, F. Berezovsky, J.S. Pala, E. Coronado, C.J. Gómez-Saiz, J.M. Clemente, A. Riou, P. Molinie, *Inorg. Chem.* 39 (2000) 3771.
- [2] E. Coronado, J.R. Galán-Mascarós, C. Giménez-Saiz, C.J. Gómez-García, C. Ruiz-Pérez, *Eur. J. Inorg. Chem.* (2003) 2290.
- [3] E. Coronado, M.C. Giménez, C.J. Gómez-García, F.M. Romero, *Polyhedron* 22 (2003) 3115.
- [4] E. Coronado, J.R. Galán-Mascarós, C.J. Gómez-García, C. Martí-Gastaldo, *Inorg. Chem.* 44 (2005) 6197.
- [5] H. Tamaki, Z.J. Zhong, N. Matsumoto, S. Kida, M. Koikawa, N. Achiwa, Y. Hashimoto, H. Okawa, *J. Am. Chem. Soc.* 114 (1992) 6974.
- [6] R. Pellaux, H. Schmalte, R. Huber, P. Fisher, T. Hauss, B. Ouladdiaf, S. Decurtins, *Inorg. Chem.* 36 (1997) 2301.
- [7] E. Coronado, J.R. Galán-Mascarós, C.J. Gómez-García, J.M. Martínez-Agudo, *Inorg. Chem.* 40 (2001) 113.
- [8] R. Andres, M. Brissard, M. Gruselle, C. Train, J. Vaissermann, B. Malezzieux, J.P. Jamet, M. Verdager, *Inorg. Chem.* 40 (2001) 4633.
- [9] E. Coronado, J.R. Galán-Mascarós, C. Martí-Gastaldo, *Inorg. Chem.* 45 (2005) 1882.
- [10] C. Mathonière, S.G. Carling, D. Yusheng, P. Day, *Chem. Soc. Chem. Commun.* (1994) 1551.
- [11] C. Mathonière, J. Nutall, S.G. Carling, P. Day, *Inorg. Chem.* 35 (1996) 1201.
- [12] E. Coronado, J.R. Galán-Mascarós, C.J. Gómez-García, J.M. Martínez-Agudo, E. Martínez-Ferrero, J.C. Waerenborgh, M. Almeida, *J. Solid State Chem.* 150 (2001) 552.
- [13] E. Coronado, J.R. Galán-Mascarós, C.J. Gómez-García, V. Laukhin, *Nature* 408 (2000) 447.
- [14] A. Alberola, E. Coronado, J.R. Galán-Mascarós, C. Giménez-Saiz, C.J. Gómez-García, *J. Am. Chem. Soc.* 125 (2003) 10774.
- [15] E. Coronado, J.R. Galán-Mascarós, C.J. Gómez-García, J. Enslin, P. Gülich, *Chem. Eur. J.* 6 (2000) 552.
- [16] S. Bénard, P. Yu, J.P. Audié, V. Rivière, R. Clément, J. Ghilhem, L. Tchertanov, K. Nakatani, *J. Am. Chem. Soc.* 122 (2000) 9444.
- [17] E. Coronado, J.R. Galán-Mascarós, C.J. Gómez-García, E. Martínez-Ferrero, M. Almeida, J.C. Waerenborgh, *Eur. J. Inorg. Chem.* (2005) 2064.
- [18] R. Sieber, S. Decurtins, H. Stoeckli-Evans, C. Wilson, D. Yufit, J.A.K. Howard, S.C. Capelli, A. Hauser, *Chem. Eur. J.* 6 (2000) 361.
- [19] S. Decurtins, H.W. Schmalte, R. Pellaux, P. Schneuwly, A. Hauser, *Inorg. Chem.* 35 (1996) 1451.
- [20] E. Coronado, M.C. Giménez, F.M. Romero, in preparation.
- [21] H.A. Goodwin, K.H. Sugiyarto, *Chem. Phys. Lett.* 139 (1987) 470.
- [22] S. Marcen, L. Lecren, L. Capes, H.A. Goodwin, J.F. Letard, *Chem. Phys. Lett.* 358 (2002) 87.

- [23] Z. Otwinowski, W. Minor, in: C.W. Carter Jr., R.M. Sweet (Eds.), *Methods in Enzymology*, vol. 276, Academic Press, New York, 1997, p. 307.
- [24] A. Altomare, M.C. Burla, M. Camali, G.L. Cascarano, C. Giacovazzo, A. Guagliardi, A.G.G. Moliterni, G. Polidori, R. Spagna, *J. Appl. Crystallogr.* 32 (1999) 115.
- [25] G.M. Sheldrick, University of Göttingen, Göttingen, Germany, 1997.
- [26] J.C. Waerenborgh, M.O. Figueiredo, J.M.P. Cabral, L.C. J. Pereira, *J. Solid State Chem.* 111 (1994) 300.
- [27] T. Buchen, P. Gütlich, K.H. Sugiyarto, H.A. Goodwin, *Chem. Eur. J.* 2 (1996) 1134.